

# Critical behavior of an even-offspringed branching and annihilating random-walk cellular automaton with spatial disorder

Géza Ódor<sup>1</sup> and Nóra Menyhárd<sup>2</sup><sup>1</sup>Research Institute for Technical Physics and Materials Science, H-1525 Budapest, P.O. Box 49, Hungary<sup>2</sup>Research Institute for Solid State Physics, H-1525 Budapest, P.O. Box 49, Hungary

(Received 16 December 2005; published 29 March 2006)

A stochastic cellular automaton exhibiting a parity-conserving class transition has been investigated in the presence of quenched spatial disorder by large-scale simulations. Numerical evidence has been found that weak disorder causes irrelevant perturbation for the universal behavior of the transition and the absorbing phase of this model. This opens up the possibility for experimental observation of the critical behavior of a nonequilibrium phase transition to absorbing state. For very strong disorder the model breaks up into blocks with exponential-size distribution and continuously changing critical exponents are observed. For strong disorder the randomly distributed diffusion walls introduce another transition within the inactive phase of the model, in which residual particles survive the extinction. The critical dynamical behavior of this transition has been explored.

DOI: [10.1103/PhysRevE.73.036130](https://doi.org/10.1103/PhysRevE.73.036130)

PACS number(s): 05.70.Ln, 82.20.Wt, 05.70.Fh

## I. INTRODUCTION

The classification of the universality classes of nonequilibrium phase transitions to absorbing states is still an open problem of statistical physics [1–3]. Reaction-diffusion (RD) models exhibiting phase transitions to absorbing states bear a particular interest since many other types of systems like surface growth, spin systems, or stochastic cellular automata can be mapped on to them. Unfortunately there has not been experimental verification of such classes except the coagulating random walk  $A+A \rightarrow A$  (CRW) in one dimension [4]. This is mainly due to the fact that the most well-known, robust directed percolation (DP) class [5,6] is sensitive to disorder [7–10], which occurs in real systems naturally. It would be very important to find some other nonequilibrium class, which proves to be less sensitive to disorder, hence would provide a candidate for experimental verification.

The study of disordered systems is a hot topic of current research of statistical physics [11]. A principal condition for the relevancy of disorder is the Harris criterion [12,13] set up for equilibrium systems and has been found to be valid in some nonequilibrium models. According to this criterion the pure critical point is stable against disorder if the spatial correlation length critical exponent  $\nu_{\perp}$  fulfills the inequality

$$d\nu_{\perp} > 2, \quad (1)$$

where  $d$  is the spatial dimensionality. However, an exception was reported very recently [14] for DP with temporal disorder. Note that for a CRW [which exhibits the same scaling behavior as the  $A+A \rightarrow \emptyset$  annihilating random walk (ARW) in one dimension (1D)] this criterion predicts relevant spatial disorder ( $\nu_{\perp}=1$ ). Still an experiment [4] did not report a measurable effect of randomness unless very strong disorder fractures the medium.

Besides the robust DP another well-known universality class is the so-called “parity-conserving” (PC) class of 1D nonequilibrium transitions. This was discovered in a one-dimensional stochastic cellular automata (CA) exhibiting  $Z_2$

symmetric absorbing states and domain walls following even-offspringed branching and annihilating random walks:  $A \rightarrow 3A$ ,  $2A \rightarrow \emptyset$  (BARW2) [15]. Later it was observed by numerical studies of other models [16–25] and field-theoretical studies [26,27] confirmed the existence of a corresponding fixed point distinct from that of DP. For a review see [28]. This class is also called the directed Ising, DP2, or generalized voter model class.

According to the Harris criterion disorder should be relevant for the critical behavior of this class [ $\nu_{\perp}=1.857(1)$  [3]]. In contrast to this a recent renormalization group (RG) study [9] did not find a strong disorder fixed point like in the case of DP. The question naturally arises if BARW2 is really insensitive to disorder or the RG method [9] is not applicable for this case. The principal aim of the present study is to answer this question. Additionally in the absorbing phase of the BARW2 model the ARW dynamics dominates, which has also been addressed in the studies [29,30]. The renormalization study of ARW with spatial randomness in the reaction rates found marginal perturbations to the fixed point of the pure system [30]. On the other hand, an exact study of the infinite reaction rate ARW with space-dependent hopping rates found nonuniversal power-law decay of the density of  $A$ -s below a critical temperature [29].

Note that in [9] the strong disorder is defined in such a way that it cannot completely block reactions or diffusion of the reactants. Therefore the so-called infinitely strong fixed point of [9] does not correspond to the blocking case. Such blocking or complete dilution was studied in a 1D toy model of a random quantum ferromagnetic Ising model [31] where continuously variable power laws were found at the phase transition point. The effect of disconnected domains in the reactions of CRW and ARW has been investigated in [32]. This study reported stretched exponential decay in the case of exponential domain-size distributions and continuously changing density decay for blocks distributed in a power-law manner. In the 1D model such complete blocking may also occur; hence, we investigate this topological effect.

## II. NEKIMCA MODEL

To study PC class transitions with disorder we have chosen a very simple stochastic cellular automaton (SCA) the NEKIMCA introduced in [21]. It is easy to show that the dual variables of spins ( $\uparrow$ ) the kinks ( $\bullet$ ) exhibit BARW2 dynamics via the synchronous spin-flip dynamics. In this SCA parity-conserving kink branching is also generated due to the synchronous spin update of neighboring sites without introducing an explicit spin-exchange reaction as in case of the NEKIM model [18]. The reactions are like the following:

random walk:  $\uparrow \uparrow \bullet \downarrow \xrightarrow{w_i} \uparrow \bullet \downarrow \downarrow$ ,

annihilation:  $\uparrow \bullet \downarrow \bullet \uparrow \xrightarrow{w_o} \uparrow \uparrow \uparrow$ ,

branching:  $\uparrow \uparrow \bullet \downarrow \downarrow \xrightarrow{w_i^2} \uparrow \bullet \downarrow \bullet \uparrow \downarrow$ .

In the NEKIMCA there are two independent variables parametrized as

$$w_i = \Gamma(1 - \delta)/2, \quad (2)$$

$$w_o = \Gamma(1 + \delta). \quad (3)$$

In the computer the state of a single spin is represented by a 1 or 0 of a 32- or 64-bit word  $s(j)$  (depending on the CPU type). Hence 32 or 64 CA samples (exhibiting different random initial conditions but the same quenched noise) are updated at once.

The following bit-parallel algorithm was used for the update of states  $s(j)$  at site  $j$ . A random number  $x(j) \in (0, 1)$  is selected with uniform distribution. If

$$x(j) < q_i(j) = w_i + \chi(j), \quad (4)$$

a spin flip, corresponding to random walk of the dual variable

$$s'(j) = [s(j+1) \wedge s(j-1)] \wedge s(j), \quad (5)$$

is written to all bits of  $s(j)'$ . Following this another uniformly distributed random number  $y(j) \in (0, 1)$  is chosen and if

$$y(j) < q_o(j) = w_o + \chi(j), \quad (6)$$

a spin flip, corresponding to annihilation of the dual variables

$$s'(j) = \{[s(j-1) \wedge s(j)] \& [s(j+1) \wedge s(j)]\} \wedge s(j), \quad (7)$$

is performed. Here  $\chi(j)$  denotes the quenched random noise variable with uniform distribution

$$\chi(j) \in (-\epsilon, \epsilon), \quad (8)$$

and  $\wedge$  and  $\&$  are the logical XOR and AND of computer words. Note that for strong disorder  $q_i(j)$  or  $q_o(j)$  may be less than 0 at a site meaning a blockade for that reaction.

A single Monte Carlo step (MCS) consists of updating all  $s'(j)$  sites with periodic boundary conditions and writing back  $s(j) = s'(j)$  for  $j \in (0, L-1)$  (throughout the paper the time is measured by MCS).

TABLE I. Numerical results for the disordered PC class transition line.

$\epsilon$	$-\delta_c$	$\alpha$	$\beta$	$z$	$\eta$
0.0	0.550(1)	0.280(6)			
0.1	0.5513(5)	0.280(6)			
0.2	0.557(1)	0.280(6)			
0.3	0.5676(1)	0.280(5)	0.95(1)	1.11(1)	0.285(5)
0.4	0.5849(1)	0.265(10)			
0.5	0.6115(4)	0.25(1)	0.84(2)	1.0(1)	0.252(6)
0.6767(2)	0.7	0.22(1)	0.80(2)		

## III. DYNAMICAL SIMULATIONS ALONG THE DISORDERED PC TRANSITION LINE

The simulations were carried out on  $L=4 \times 10^4 - 10^5$  sized systems with periodic boundary conditions. The initial states were randomly half-filled lattices, and the density of kinks is followed up to  $10^7 - 10^8$  MCS. We started the exploration of the  $(\delta, \epsilon)$  phase diagram by determining the phase transition of the impurity-free ( $\epsilon=0$ ) case with  $\Gamma=1$ . This was located at  $\delta_c = -0.550(1)$  as a power-law decay of the kink density,

$$\rho \propto t^{-\alpha}, \quad (9)$$

with exponent  $\alpha=0.28(1)$ . This is in good agreement with the PC class value [21]. Next we introduced the quenched disorder and determined  $\delta_c$  for different  $\epsilon$  values. Table I and Fig. 1 show the results. As one can see the disorder moves the transition point in such a way that the size of absorbing phase increases along the  $-\delta$  axis.

Weak disorder ( $\epsilon < w_o$ ) seems to be irrelevant (see Fig. 2). The line corresponding to  $\delta=0.5675$  can well be described by a power law from  $10^3 < t < 10^8$  MCS (5 decades) with

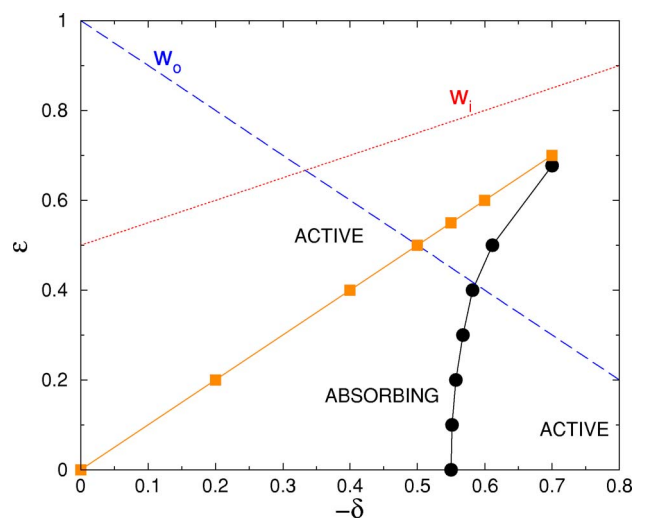


FIG. 1. (Color online) Phase diagram of the disordered NEKIMCA for negative  $\delta$ . Bullets correspond to the disordered PC class transition points, squares to the freezing transition (lines are a guide for the eye only). The dashed line shows  $w_o$ , while the dotted line denotes  $w_i$ .

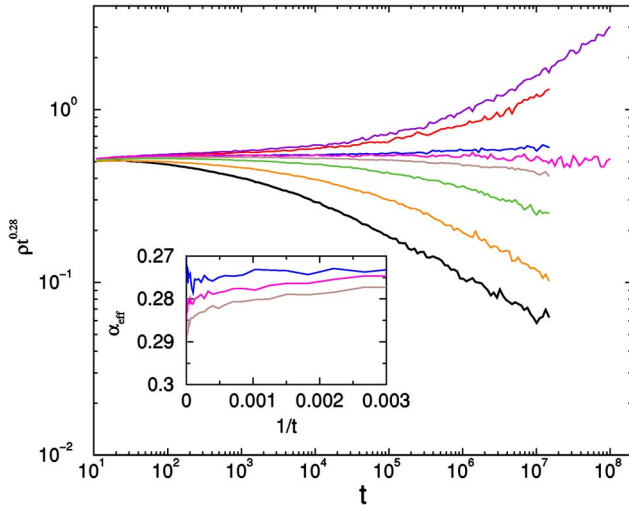


FIG. 2. (Color online) Density decay of NEKIMCA for  $\epsilon=0.3$ ,  $\Gamma=1$  for different  $\delta=0.571, 0.57, 0.568, 0.5675, 0.567, 0.565, 0.56, 0.55$  (from top to bottom). The insert shows the local slopes for  $\delta=0.568, 0.5675, 0.567$  (from top to bottom).

exponent  $\alpha=0.28$ . The local slopes (effective exponents) of the kink density decay are defined as

$$\alpha_{eff}(t) = \frac{-\ln[\rho(t)/\rho(t/m)]}{\ln(m)} \quad (10)$$

(where we used  $m=2$ ). At the critical point the  $\alpha_{eff}(t)$  curve exhibits a straight-line shape for  $t \rightarrow \infty$ , while in subcritical (supercritical) cases  $\alpha_{eff}(t)$  curves veer down (up), respectively. One can read off  $\alpha_{eff} \rightarrow \alpha=0.28(1)$  in a perfect agreement with the PC class value. Similar results are obtained for  $\epsilon=0.1, 0.2, 0.4$  and summarized in Table I.

To confirm these results we run cluster-spreading simulations from a single active seed (one kink, odd sector) and measured the number of particles  $[N(t)]$  and the diameter of clusters  $[R(t)]$ . At the critical point these are expected to scale as

$$N(t) \propto t^\eta, \quad R(t) \propto t^{z/2}. \quad (11)$$

As Fig. 3 shows both quantities exhibit power-law behavior with PC class exponents  $\eta=0.285(5)$  and  $z=1.11(1)$  [17,28].

Finally we performed steady-state simulations in the active phase at  $\epsilon=0.3$ . We followed the density of kinks in many realizations until saturation is reached and averaged in a time window following that point. The steady-state density in the active phase at a critical phase transition is expected to scale as

$$\rho(\infty, \delta) \propto |\delta - \delta_c|^\beta. \quad (12)$$

Using the local slopes method one can get a precise estimate for  $\beta$  as well as for the corrections to scaling,

$$\beta_{eff}(\delta_i) = \frac{\ln \rho(\infty, \delta_i) - \ln \rho(\infty, \delta_{i-1})}{\ln(\delta_i) - \ln(\delta_{i-1})}, \quad (13)$$

where we used the  $\delta_c$  value determined before. The local

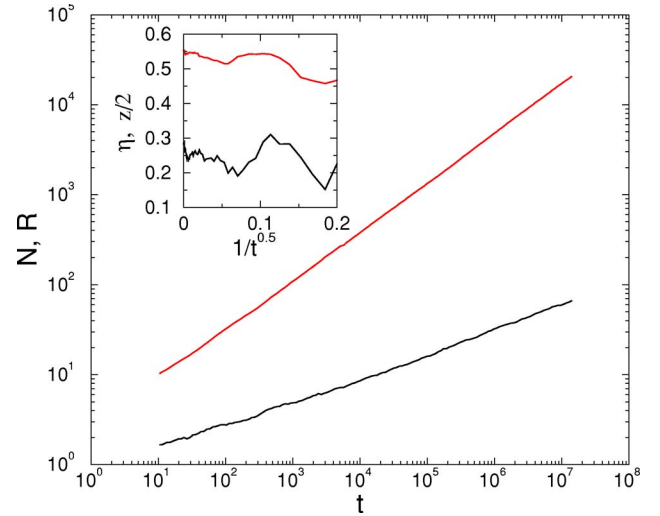


FIG. 3. (Color online) Spreading in NEKIMCA for  $\epsilon=0.3$ ,  $\Gamma=1$ ,  $\delta_c=-0.5679$ . The inset shows the corresponding local slopes.

slopes analysis resulted in  $\beta_{eff} \rightarrow \beta=0.95(1)$  in agreement with the PC class value again [25] (see Fig. 4).

#### Annihilation blocking on the disordered PC transition line

In the inactive phase and at the critical point depletion of kinks dominates via the  $AA \rightarrow \emptyset$  annihilation. However, for strong enough disorder active domains of arbitrary sizes may also emerge due to the exponential distribution of such events. The contribution of these such large regions can be estimated as in [13] with the difference that for the PC class even the absorbing phase decays algebraically; i.e., one does not have exponential decay that could slow down to stretched exponential at some “clean critical point” as in the DP case. The probability  $p_a$  for finding a rare region of size  $l_a$  is

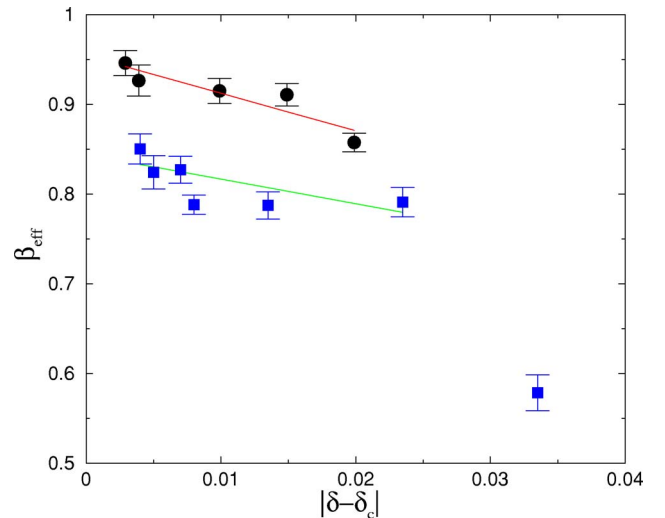


FIG. 4. (Color online) Effective order parameter exponent results on the disordered PC class line for  $\epsilon=0.3, 0.5$  (top to bottom). Lines correspond to a linear fit.

$$p_a \propto \exp(-ql_a), \quad (14)$$

where  $q \propto w_i^2 - w_o + \epsilon$  is the probability that a site is active. The long-time kink decay density is dominated by these rare regions. For long times any finite region decays exponentially hence

$$\rho(t) \propto \int dl_a l_a p_a \exp[-t/\tau(l_a)], \quad (15)$$

where  $\tau(l_a)$  is the characteristic decay time of a size of region of size  $l_a$ . The average lifetime of such active regions grows as

$$\tau(l_a) \propto \exp(al_a) \quad (16)$$

because a coordinated fluctuation of the entire region is required to take it to the absorbing state. The saddle-point analysis of (15) as in [13] results in power-law decay

$$\rho(t) \propto t^{-p_a/a}. \quad (17)$$

Hence one may expect continuously changing decay exponents either as the effect of rare active regions or as the effect of high diffusion barriers [29].

As we discussed in the previous section we did not see the occurrence of such continuous-decay variables for weak disorder. However, by going above  $\epsilon > \sim 0.4$  the situation changes and we begin to see deviation from the pure PC decay behavior (see Table I). The effect of disorder becomes drastic. By increasing  $\epsilon$  above  $w_o$  the  $q_o$  reaction probabilities may become zero at certain sites randomly (with probability  $p_w$ ) and the kink annihilation is blocked at those sites. From annihilation reaction point of view the systems falls apart to  $l$  blocks with an exponential probability distribution

$$p(l) = p_w p_{nw}^l, \quad (18)$$

where the no-wall probability  $p_{nw}$  is related to  $\epsilon$  according to our algorithm as  $p_{nw} = 1 - p_w = 1 - (\epsilon - w_o)$  is set. This means that neighboring kinks cannot even annihilate at the block boundary points which may cause relevant perturbation to the critical behavior.

As Fig. 5 shows for  $\epsilon=0.5$  the phase transition occurs at  $\delta_c = -0.6115(3)$  and the density decay exponent is smaller than the PC class value:  $\alpha=0.25(1)$ . For  $\delta=-0.7$  and  $\epsilon_c = 0.677(1)$ , it is even smaller,  $\alpha=0.22(1)$ , suggesting continuously changing exponents along this transition line by increasing  $\epsilon$ . Similarly the steady-state exponent  $\beta$  and the spreading exponent  $z$  change in this region (see Table I and Fig. 3).

#### IV. DYNAMICAL SIMULATIONS IN THE INACTIVE PHASE

In the inactive phase the annihilating random walk dominates, in which for pure systems the density decays asymptotically as a power law [33]:

$$\rho \propto t^{-1/2}, \quad (19)$$

hence, one can check the effect of disorder for this process. As one can see on Fig. 6 the disorder does not change this

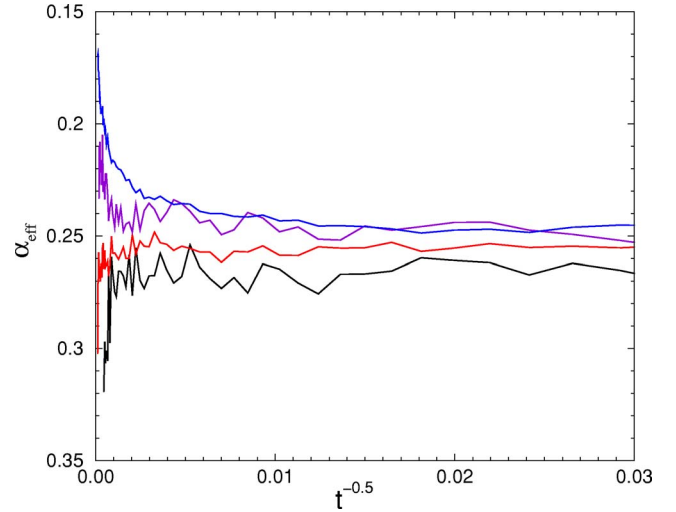


FIG. 5. (Color online) Effective  $\alpha$  in the strong-disorder region of the disordered PC class transition line ( $\epsilon=0.5$ ),  $-\delta_c=0.613, 0.612, 0.611, 0.609$  (top to bottom).

behavior for small  $\epsilon$ ; the  $\rho(t)t^{1/2}$  curves level off. For larger  $\epsilon$ , however, the deviations from the law (19) is observable for long time. Following a transient region, which is faster than (19) and characteristic of an ARW with finite reaction rates [34], the decay slows down. For example, for  $\epsilon=0.57$  and  $\delta=-0.6$  power-law fitting for  $t > 10^6$  MCS results in  $\alpha = 0.43(1)$ , while for  $\epsilon=0.48$  and  $\delta=-0.5$  we obtained  $\alpha = 0.46(1)$ . These  $\epsilon$ -dependent  $\alpha$  values are in agreement with the results of [29], where continuously changing power-law exponents are determined below a critical temperature in the case of exponentially distributed diffusion barrier heights.

#### V. DYNAMICAL SIMULATIONS OF THE FREEZING TRANSITION

As one can see in Fig. 1 for negative  $\delta$  values the PC class transition line does not cross the  $w_i$  line, suggesting that the diffusion and branching reactions are not blocked. However,

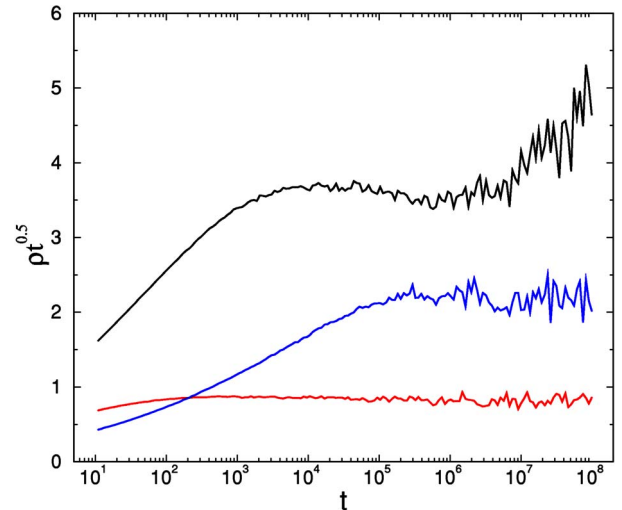


FIG. 6. (Color online) Density decay in the inactive phase at coordinates  $(\delta=-0.6, \epsilon=0.57)$ ,  $(\delta=-0.5, \epsilon=0.3)$ ,  $(\delta=-0.525, \epsilon=0.1)$  (top to bottom).

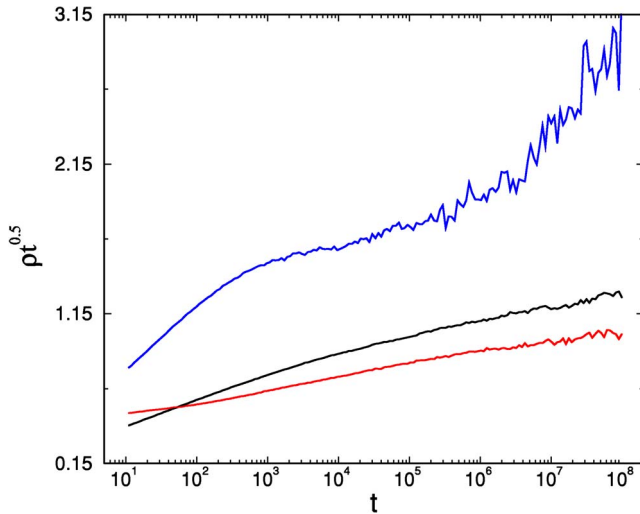


FIG. 7. (Color online) Density decay on the freezing transition line for  $\epsilon=0.6, 0.4, 0.2$  (top to bottom).

due to the parallel computer algorithm we used in the case of strong disorder ( $\epsilon \geq 1 - w_o$ ),  $q_o$  may become 1 at certain sites and hence a random walk move is immediately overwritten by the CA update (7) at these sites. As a consequence in the absorbing phase (above the disordered PC transition line) the diffusion is blocked. Again the system falls apart to blocks with closed diffusion boundaries. As the depletion goes on kinks cannot leave the blocks to interact with others in neighboring ones and “frozen” steady states emerge for  $\epsilon > -\delta$ . Note, however, that the system is not completely frozen; kinks cannot only diffuse within the blocks, but branching may occur with (small probability) followed by a quick annihilation. In any case the residual density remains small.

We run dynamical simulations on the freezing transition line, and as Fig. 7 shows the density decay is slower than the square-root law of ARW (19) and changes continuously along the freezing transition line (see Table II). However, for  $\epsilon \leq 0.5$  this deviation can be interpreted as a (logarithmic) correction to scaling. For  $\epsilon > 0.5$  even the  $w_o$  (annihilation) reactions are blocked and the deviation from (19) is strong. We repeated this simulation on a system with different size ( $L=10^4$ ), but did not see any size dependence.

The spreading exponent  $z$  changes similarly along the freezing transition line. It is close to  $z=1$  for  $\epsilon \leq 0.5$  and deviates it significantly for  $\epsilon > 0.5$  (see Fig. 8). The average number of kinks  $[N(t)]$  evolves to a small constant value as  $t \rightarrow \infty$  ( $\eta=0$ ) all along the freezing transition line. This value changes continuously by increasing the disorder strength.

TABLE II. Numerical results for the freezing transition line.

$\epsilon$	$-\delta_c$	$\alpha$	$\beta$	$z$	$N(\infty)$
0.2	0.2	0.47(3)	1.00(5)	0.95(5)	1.031(1)
0.4	0.4	0.47(3)		0.95(5)	1.275(5)
0.5	0.5	0.43(1)		1.0(2)	1.85(5)
0.6	0.6	0.41(1)	0.75(3)	0.76(2)	3.75(5)
0.7	0.7	0.39(1)	0.68(4)	0.72(2)	14(1)

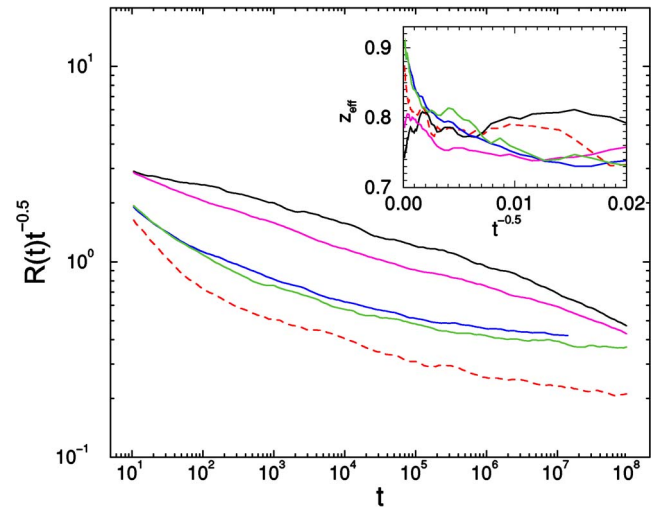


FIG. 8. (Color online) Spreading in NEKIMCA along the freezing transition line  $\epsilon=0.7, 0.6, 0.0, 0.2, 0.125$  (top to bottom). The  $\epsilon=0, 0.125$  data correspond to  $\Gamma=0.5$ , the others to  $\Gamma=1$ . The  $\epsilon=0.125$  line corresponds to  $\delta=0.5$ , the others to  $\epsilon=-\delta$ . The inset shows the corresponding local slopes.

For  $\epsilon \leq 0.2$  only a single kink survives [ $N(\infty) \simeq 1$ ], while for other values see Table II.

In the frozen (active) phase in the long-time limit pairs within the same block annihilate and basically lonely kinks are wandering in confined regions of sizes  $l$  (local  $A \rightarrow 3A \rightarrow A$  reactions are also permitted with a small probability). Therefore the density of frozen kinks depends on the density of blocks, hence on  $\epsilon$ . The concentration of blocks  $c_b$  can be expressed with the average length  $\langle l \rangle$  of blocks as

$$\rho \propto c_b \propto \langle l \rangle^{-1}. \quad (20)$$

For the exponential block size distribution (18) the average block size is

$$\langle l \rangle = [-\ln(p_{nw})]^{-1}, \quad (21)$$

with the no-wall probability

$$p_{nw} = 1 - p_w = 1 - (w_o + \epsilon - 1) = 2 - \epsilon - w_o. \quad (22)$$

The kink density is

$$\rho \propto -\ln(2 - \epsilon - w_o), \quad (23)$$

which for small wall probability  $p_w$  has the leading-order singularity

$$\rho \propto p_w. \quad (24)$$

This means that in the frozen phase  $\beta=1$ . The simulations confirm this. For  $\epsilon < 0.5$ , where only diffusion traps are present the  $\beta \sim 1$  indeed (see Table II and Fig. 9). For  $\epsilon \geq 0.5$  where annihilation is also blocked the exponent  $\beta$  decreases by increasing  $\epsilon$  (see Table II).

We have also investigated the phase space for positive  $\delta$  (with  $\Gamma=0.5$ ) where  $\epsilon > w_i$  causes a direct freezing transition via diffusion traps in the absorbing phase. The density decay

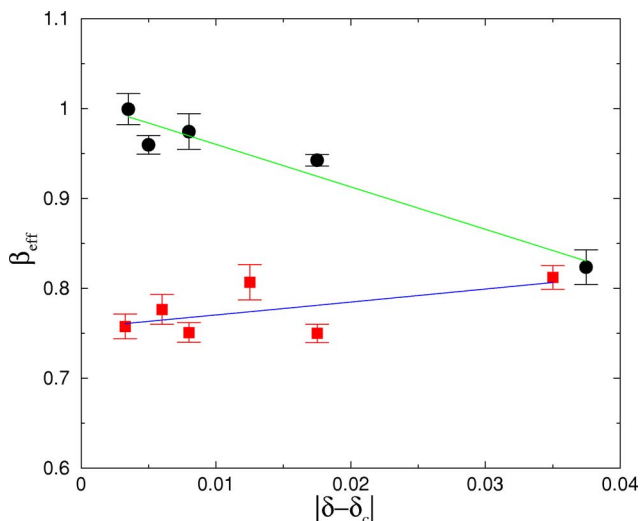


FIG. 9. (Color online) Effective order parameter exponent results on the freezing transition line for  $\epsilon=0.2, 0.6$  (top to bottom). Lines correspond to a linear fit.

simulations (see Fig. 10) show small deviations from the square-root law of ARW (19), which can be interpreted as corrections to scaling.

## VI. DISCUSSION

We have investigated the phase diagram of the NEKIMCA as the function of quenched disorder with large-scale simulations. We have chosen NEKIMCA, a very simple SCA, which is known to exhibit PC class transition of kinks to absorbing states. We determined static and dynamic exponents ( $\alpha, \beta, \eta, z$ ) at several points along the phase transition line and in the inactive phase. The main consequence of this survey is that weak disorder does not change the scaling behavior of the quantities studied. This supports the results of a recent real-space RG study [9] but contradicts the Harris criterion.

A possible resolution of this contradiction could be the study of the distribution of the critical-point coordinates over the ensemble of samples of size  $L$ . According to recent progresses in the finite-size scaling theory of disordered systems, thermodynamic observable are not self-averaging at critical points when the disorder is relevant in the Harris criterion sense [35–40]. This lack of self-averageness at criticality is directly related to the distribution of pseudocritical temperatures  $T_c(i, L)$  over the ensemble of samples ( $i$ ) of size  $L$ . This has been shown numerically in the case of a wetting transition of a polymer chain with quenched disorder [41]. An interesting further direction of research would be the study of those distributions for nonequilibrium systems like for NEKIMCA.

For weak disorder ( $\epsilon < \approx 0.4$ ) we did not see deviations from the asymptotic square-root power law (19) in the inactive phase. However, for stronger disorder a continuously changing density decay exponent ( $\alpha$ ) was observed. This

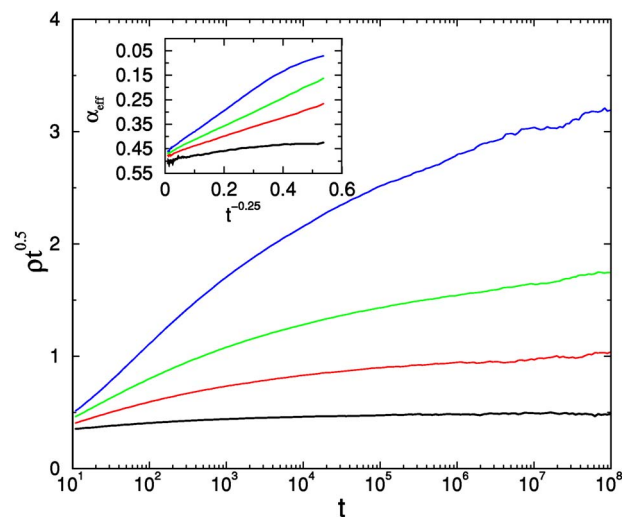


FIG. 10. (Color online) Density decay in NEKIMCA for positive  $\delta$  along the freezing transition line  $\epsilon=0.075, 0.125, 0.175, 0.25$  (top to bottom). The inset shows the corresponding local slopes.

corroborates a former RG study [30] for ARW's with site-dependent reaction rates and an exact calculation for the infinite-reaction-rate ARW with disordered diffusion traps [29].

Very strong disorder in our model may introduce complete blocking of reactions or diffusion with exponential domain-size distribution. If the system becomes segmented by diffusion walls, a freezing transition to fluctuating states occurs. In this case in odd-parity blocks residual particles remain active. Large-scale simulations suggest that this kind of disorder is marginal; the density decay slows down from the power law (19) by a logarithmic correction or changes continuously if the annihilation is blockaded too. In the frozen phase the concentration of residual kinks increases logarithmically, with  $\beta_{\text{eff}} \rightarrow 1$  asymptotically. This is in agreement with the results of [32], who considered the ARW model with complete blockades. However, we did not see the crossover to stretched exponential decay reported in [32] for long time, but rather the decay slows down in our model. This is due to the fact that in our model in the frozen state not only do blockades exist, but reaction and diffusion probabilities are randomized, which can introduce slower power laws [13,29,30].

In the region of the phase diagram where the disorder is so strong that the annihilation reaction becomes segmented we found continuously changing exponents along both the disordered PC and the freezing transition lines.

## ACKNOWLEDGMENTS

We thank F. Iglói and G. M. Schütz for the useful comments. Support from Hungarian research funds OTKA (Grant No. T046129) is acknowledged. The authors thank the access to the NIFI Cluster-GRID, LCG-GRID, and the Supercomputer Center of Hungary.

- [1] For references, see J. Marro and R. Dickman, *Nonequilibrium Phase Transitions in Lattice Models* (Cambridge University Press, Cambridge, England, 1999).
- [2] For a review, see H. Hinrichsen, *Adv. Phys.* **49**, 815 (2000).
- [3] For a recent review see G. Ódor, *Rev. Mod. Phys.* **76**, 663 (2004).
- [4] R. Kroon, H. Fleurent, and R. Sprik, *Phys. Rev. E* **47**, 2462 (1993).
- [5] W. Kinzel, in *Percolation Structures and Processes*, edited by G. Deutscher, R. Zallen, and J. Adler (Hilger, Bristol, 1983); H. K. Janssen, *Z. Phys. B: Condens. Matter* **42**, 151 (1981); P. Grassberger, *ibid.* **47**, 365 (1982).
- [6] P. Grassberger, *Z. Phys. B: Condens. Matter* **47**, 365 (1982).
- [7] H. K. Janssen, *Phys. Rev. E* **55**, 6253 (1997).
- [8] R. Cafiero, A. Gabrielli, and M. A. Muñoz, *Phys. Rev. E* **57**, 5060 (1998).
- [9] J. Hooyberghs, F. Iglói, and Carlo Vanderzande, *Phys. Rev. E* **69**, 066140 (2004).
- [10] T. Vojta and M. Dickison, *Phys. Rev. E* **72**, 036126 (2005).
- [11] For a recent review, see F. Iglói and C. Monthus, *Phys. Rep.* **412**, 277 (2005).
- [12] A. B. Harris, *J. Phys. C* **7**, 1671 (1974).
- [13] A. J. Noest, *Phys. Rev. Lett.* **57**, 90 (1986); *Phys. Rev. B* **38**, 2715 (1988).
- [14] I. Jensen, *J. Phys. A* **38**, 1441 (2005).
- [15] P. Grassberger, F. Krause, and T. von der Twer, *J. Phys. A* **17**, L105 (1984).
- [16] H. Takayasu and A. Yu. Tretyakov, *Phys. Rev. Lett.* **68**, 3060 (1992).
- [17] I. Jensen, *Phys. Rev. E* **50**, 3623 (1994).
- [18] N. Menyhárd, *J. Phys. A* **27**, 6139 (1994).
- [19] M. H. Kim and H. Park, *Phys. Rev. Lett.* **73**, 2579 (1994).
- [20] D. Zhong and D. ben-Avraham, *Phys. Lett. A* **209**, 333 (1995).
- [21] N. Menyhárd and G. Ódor, *J. Phys. A* **28**, 4505 (1995).
- [22] K. E. Bassler and D. A. Browne, *Phys. Rev. Lett.* **77**, 4094 (1996).
- [23] H. Hinrichsen, *Phys. Rev. E* **55**, 219 (1997).
- [24] D. Zhong, D. ben-Avraham, and M. A. Muñoz, *Eur. Phys. J. B* **35**, 505 (2003).
- [25] G. Ódor and A. Szolnoki, *Phys. Rev. E* **71**, 066128 (2005).
- [26] J. L. Cardy and U. C. Täuber, *Phys. Rev. Lett.* **77**, 4780 (1996); *J. Stat. Phys.* **90**, 1 (1998).
- [27] O. Al Hammal, H. Chaté, B. Delmotte, I. Dornic, and M. A. Muñoz, *Phys. Rev. Lett.* **95**, 100601 (2005).
- [28] N. Menyhárd and G. Ódor, *Braz. J. Phys.* **30**, 113 (2000).
- [29] G. M. Schütz and K. Mussawisade, *Phys. Rev. E* **57**, 2563 (1998).
- [30] P. Le Doussal and C. Monthus, *Phys. Rev. E* **60**, 1212 (1999).
- [31] D. S. Fisher, *Physica A* **263**, 222 (1999).
- [32] C. Mandache and D. ben-Avraham, *J. Chem. Phys.* **112**, 7735 (2000).
- [33] B. P. Lee, *J. Phys. A* **27**, 2633 (1994).
- [34] L. Braunstein, H. O. Martin, M. D. Grynberg, and H. E. Roman, *J. Phys. A* **25**, L255 (1992).
- [35] S. Wiseman and E. Domany, *Phys. Rev. E* **52**, 3469 (1995).
- [36] A. Aharony and A. B. Harris, *Phys. Rev. Lett.* **77**, 3700 (1996).
- [37] F. Pázmándi, R. T. Scalettar, and G. T. Zimányi, *Phys. Rev. Lett.* **79**, 5130 (1997).
- [38] S. Wiseman and E. Domany, *Phys. Rev. Lett.* **81**, 22 (1998); *Phys. Rev. E* **58**, 2938 (1998).
- [39] A. Aharony, A. B. Harris, and S. Wiseman, *Phys. Rev. Lett.* **81**, 252 (1998).
- [40] K. Bernardet, F. Pázmándi, and G. G. Batrouni, *Phys. Rev. Lett.* **84**, 4477 (2000).
- [41] C. Monthus and T. Garel, *J. Stat. Mech.: Theory Exp.* P12011 (2005).